THE ELECTRON AND MAGNETIC FIELD ENERGIES IN THE EAST LOBE OF THE RADIO GALAXY FORNAX A, MEASURED WITH XMM-NEWTON.

N. Isobe[1], K. Makishima[1,2], M. Tashiro[3], K. Ito[3], N. Iyomoto[4], and H. Kaneda[5]

[1]The Institute of Physical and Chemical Research (RIKEN), 2-1 Hirosawa, Wako, Saitama, 351-0198, Japan
[2]Department of Physics, University of Tokyo, 7-3-1, Hongo, Bunkyo, 113-0033, Japan
[3]Department of Physics, Saitama University, Shimo-Okubo, Saitama, 338-8570, Japan.
[4]Laboratory for High Energy Astrophysics, Code 662, NASA Goddard Space Flight Center, Greenbelt, MD 20771, USA
[5]Institute of Space and Astronautical Science, Japan Aerospace Exploration Agency (ISAS/JAXA), 3-1-1, Yoshinodai, Sagamihara, Kanagawa, 229-8510, Japan

ABSTRACT

In an XMM-Newton observation of the east lobe of nearby radio galaxy Fonrax A, we have significantly detected the diffuse X-ray emission, which was originally discovered by *ASCA* and *ROSAT*. The X-ray spectrum of the diffuse emission is described by a single power-law model, modified with the Galactic absorption toward the object. The best-fit X-ray photon index, $1.62^{+0.25}_{-0.15}$, agrees well with the synchrotron radio index, 1.68 ± 0.05, between 29.9 MHz and 5 GHz. Therefore, the inverse Compton interpretation for the diffuse X-ray emission is justified. A comparison between the radio and X-ray flux densities gives a moderate electron-energy dominance over in the east lobe of Fornax A, in spite of the dormancy of its nucleus. We also reexamined the ASCA result on the west lobe, to find that both lobes share the similar physical condition.

Key words: radiation mechanisms: non-thermal — magnetic fields — X-rays: galaxies — radio continuum: galaxies — galaxies: individual (Fornax A) .

1. INTRODUCTION

Inverse Compton (IC) X-ray emission associated with the lobes of radio galaxies and quasars is a very useful probe to investigate the energetics in jet-lobe systems, once the seed photon source is usually identified with the cosmic microwave background (CMB) radiation (Harris & Grindlay, 1979), or infra-red photons from the nucleus (Brunetti et al., 1997). The recent detections of the these lobe-IC X-rays with *ASCA*, *Chandra* and *XMM-Newton* frequently claim an electrons dominance of $u_{\rm e} \sim 10 u_{\rm m}$ in the lobes (Croston et al., 2005; Isobe et al., 2005), where $u_{\rm e}$ and $u_{\rm m}$ is energy density of electrons and magnetic fields in the lobes, respectively.

The lobe-IC X-ray emission was originally discovered from the nearby radio galaxy Fornax A. with *ROSAT* (Feigelson et al., 1995) and *ASCA* (Kaneda et al., 1995). Fornax A is the fourth brightest radio source all over the sky in the GHz band, located at the southern hemisphere. Although the radio images of Fornax A show a prototypical double-lobe morphology (Ekers et al., 1983), which naturally suggests a past activity of the jets from the nucleus, recent X-ray observations indicate a current dormancy of the nucleus (Iyomoto et al., 1998; Kim & Fabianno, 2003). Therefore, Fornax A is one of the most important target to study the evolution of energetics in lobes of radio galaxies, associated with the activity of the jets from the nucleus. Actually, the *ASCA* result (Kaneda et al., 1995; Tashiro et al., 2001) dose not conflict with an equipartition between $u_{\rm e}$ and $u_{\rm m}$, though with lightly large errors.

We report here, the *XMM-Newton* observation of Fornax A, in which the IC X-ray emission from the east lobe was confirmed with significantly improved signal statistics. We adopted the distance to Fornax A to be 18.6 Mpc (Madore et al., 1999), At the distance, $1'$ corresponds to a physical size of 5.41 kpc.

2. OBSERVATION AND RESULTS

We conducted a 60 ksec observation of the east lobe of Fornax A, and obtained about 26 ksec of good exposure for the MOS camera. However, we diceded to reject all the PN data, because the background was found to be unstable, even after we carefully removed so-called background flare periods. The details on the data reduction and the background rejection will be presented elsewhere (Isobe et al., submitted to ApJ).

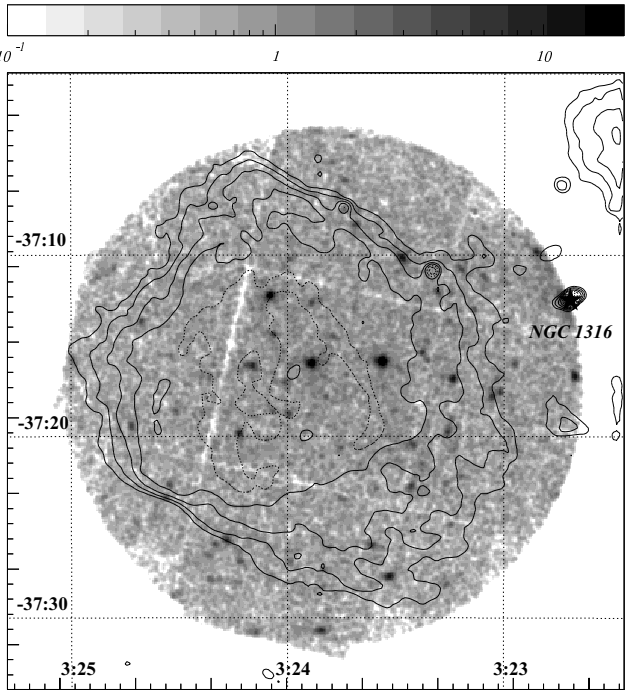

Figure 1. The 0.3 – 10 keV MOS image of the east lobe of Fornax A, smoothed with a two dimensional Gaussian of $5''$ *radius. The backgound is not subtracted. The 1.5 GHz VLA contour image (Fomalont et al., 1989) is overlaid. The center of the host galaxy, NGC1316, is shown with the filled star at the edge of the MOS VOV. The east lobe is fully contained in the MOS field of view.*

2.1. X-ray Image

We show a raw 0.3 – 10 keV MOS image in the left panel of Figure 1, The 1.5 GHz radio image (Fomalont et al., 1989) is superposed with contours on the X-ray image, to visualize that the east lobe is fully contained within the MOS field of view (FOV). However, the center of the host galaxy, NGC 1316, locates near the FOV edge. We have detected, in total, 59 X-ray sources in this image, almost all of which were not able to be resolved with the *ASCA*.

In order to search for the diffuse X-ray emission associated with the east lobe, we removed all the detected point sources. The right panel of Figure 2 shows the source-removed, background-subtracted MOS image in 0.3 – 10 keV. The image is heavily smoothed with a two dimensional Gaussian of $\sigma = 1'$, after the exposure correction is performed. Diffuse X-ray emission has been clearly detected almost all over the east lobe.

2.2. X-ray spectrum

The MOS spectrum of the east lobe, integrated within the smaller circle ($10'$ raduis) in the right panel of Figure 1, is shown in Figure 3. The X-ray signals are highly significant (about 24σ) in the 0.3 – 6 keV range. We removed all the detected point sources in the same manner as for the X-ray image. The spectrum appears relatively featureless and hard. t is successfully reproduced by a single power-law (PL) model modified with a free absorption. The best-fit spectral parameteds are summarised in Table 1 (Fit 1). The photon index becomes $\Gamma_{\rm X} = 1.62^{+0.24}_{-0.15}$, which is consistent with the *ASCA* result (Kaneda et al., 1995). The flux density at 1 keV, $S_{\rm 1keV} = 86^{+18}_{-9}$ nJy, becomes slightly smaller than the *ASCA* result of 110 ± 50 nJy. The absorption column density coincides with the Galactic value toward Fornax A, 2.06×10^{20} cm^{-2} (Stark et al., 1992), within the sta-

Table 1. The best-fit PL spectral parameters

Parameter	Fit1	Fit2
$N_{\rm H}(10^{20}$ cm$^{-2})$	$1.2\ ^{+5.5}_{-1.2}$	$2.4\ ^{+2.8}_{-2.4}$
$\Gamma_{\rm X}$	$1.62\ ^{+0.24}_{-0.15}$	1.68 (fix)
$S_{\rm 1keV}$(nJy)^a	$86\ ^{+18}_{-9}$	$90\ ^{+8}_{-9}$
$F_{\rm X}(10^{-13}$ erg cm^{-2} s$^{-1})^b$	$5.9\ ^{+0.6}_{-0.5}$	
$L_{\rm X}(10^{40}$ erg s$^{-1})^c$	$2.4\ ^{+0.3}_{-0.2}$	
χ^2/d.o.f	26.5/29	26.7/30

^{a}Flux density at 1 keV. ^{b}Absorption-corrected flux in 0.5 – 5 keV. ^{c}Absorption-corrected luminosity in 0.5 – 5 keV.

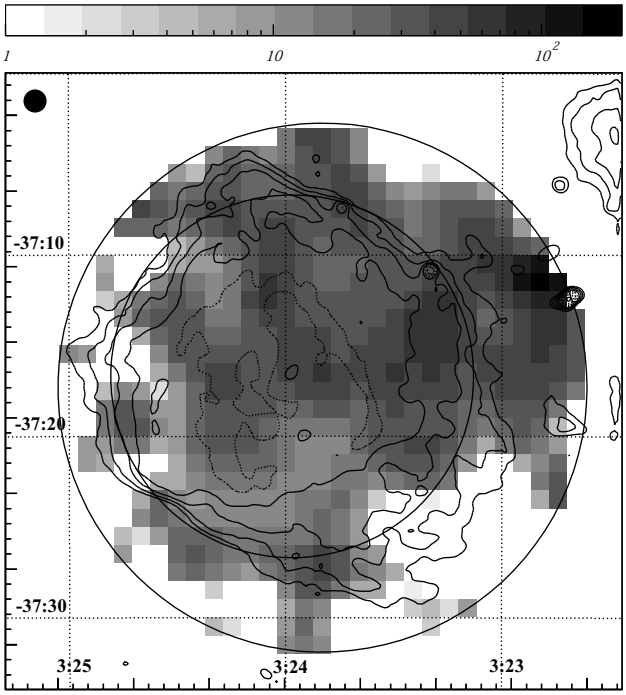

Figure 2. The background-subtracted MOS image in 0.3 – 10 keV, which is heavily smoothed with a two dimensional Gaussian of $1'$ *radius. The exposure is corrected, after all the detected X-ray sources (circles of 36" radius) are rejected. The two colid circles indicate the MOS FOV and the integration region of the spectrum of the east lobe. The same contour radio image is overlaid.*

tistical uncertainty. Thanks to the careful removal of contaminating point sources, these parameters can be considered to represent the "true" spectrum of the diffuse X-ray emission of the east lobe.

3. DISCUSSION

We show the radio and X-ray spectral energy distribution of Fornax A in Figure 4 (reference therein). The radio spectrum between 29.9 MHz and 5 GHz is almost successfully descrived by a PL model with a photon index of $\Gamma_{\rm R} = 1.68 \pm 0.05$. Although we have found only two data points for the east lobe at 1.4 and 2.7 GHz, the index between the two data points agrees well with $\Gamma_{\rm R}$, as shonw with the dashed line in Figure 4. Then, we think that this $\Gamma_{\rm R}$ also represents the radio spectrum of the east lobe. The best-fit X-ray index $\Gamma_{\rm X}$ of the east lobe is consistent with $\Gamma_{\rm R}$, within the statistical uncertainty. Therefore, we have concluded that the diffuse X-ray emission is of IC origin, and the seed photon source is of no doubt the CMB radiation, as already discussed in detail by KEA95.

According to Harris & Grindlay (1979), we estimated the physical parameters in the east lobe of Fornax A. We here, re-evaluated the X-ray flux density at 1 keV by the PL fitting with a photon index fixed at $\Gamma_{\rm R} = 1.68$ (see Fit 2 in Table 1). The relevant parameters are summarised in Table 2. We have safely rejected an energy equipartition between the electrons and magnetic field, and instead, revealed a moderate electron dominance of $u_{\rm e}/u_{\rm m} \sim 5$ in the east lobe. Correspondingly, the magnetic field is found to be about 20% weaker than the equipartition value $B_{\rm me}$.

The *ASCA* value of the IC X-ray index of the west lobe, $\Gamma_{\rm X} = 1.74 \pm 0.1$ (Tashiro et al., 2001), well coincides with the radio synchrotron index, $\Gamma_{\rm R} = 1.68$. But Tashiro et al. (2001) adopted the radio index of $\Gamma_{\rm R} = 1.9 \pm 0.2$, based only on three data points between 843 MHz and 2.7 GHz, in the evaluation of the energetics in the west lobe. Therefore, we re-evaluated $u_{\rm e}$ and $u_{\rm m}$ in the west lobe of Fornax A, by using $\Gamma_{\rm R} = 1.68$. As shown in Table 2, it is found that both lobes share similar physical condition.

The nucleus of Fornax A is reported to have been already faded out (Iyomoto et al., 1998; Kim & Fabianno, 2003). This means that the electrons and magnetic field in the lobes of Fornax A are thought to be no longer supplied with sufficient energy by the jets from the nucleus. Therefore, it reasonable that both $u_{\rm e}$ and $u_{\rm m}$ in the lobes of Fornax A is found to be lower than the typical values in the lobes of radio galaxies; $u_{\rm e} = 10^{-12\sim-9}$ erg cm^{-3} and $u_{\rm m} = 10^{-13\sim-10}$ erg cm^{-3} (Croston et al., 2005; Isobe

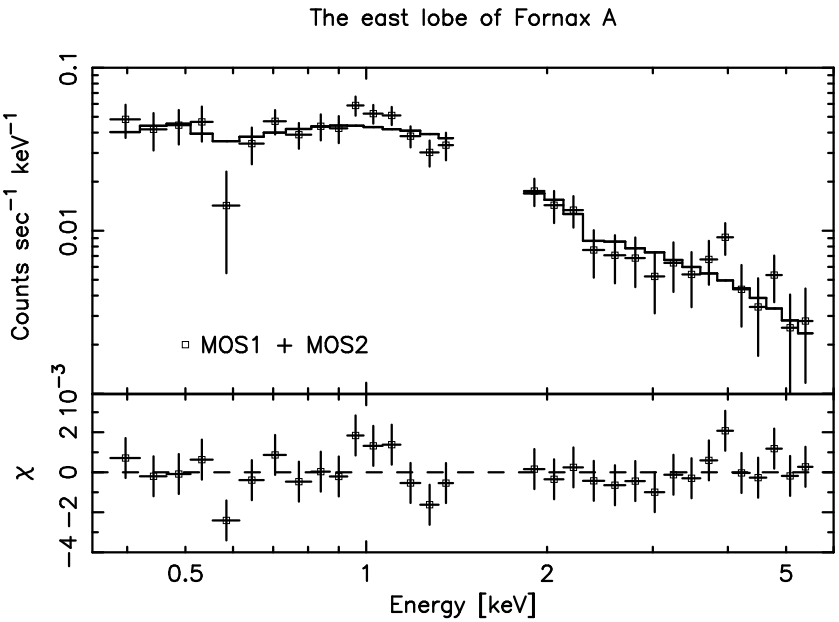

Figure 3. The background-subtracted MOS spectrum of the east lobe of Fornax A, in the 0.3 – 6 keV range. The data between 1.4 and 1.8 keV are rejected, due to a severe contamination from a prominent instrumental background feature. The histogram indicates the best-fit PL model spectrum modified with a free absorption (Fit1 in Table 1).

et al., 2005). However, we have confirmed the electron dominance even in the lobes of Fornax A, with a relatively moderate degree of $u_{\rm e}/u_{\rm m} \sim 5$. Because the electrons in the lobes of Fornax A currently only lose their energy continuously through IC X-ray and synchrotron radio radiation, they will evolve to achieve the equipartition condition within a few Gyr, considering the cooling time of electrons in the lobes.

The *ASCA* result (Tashiro et al., 2001) also indicated a rim-strengthened magnetic field feature in the west lobe of Fornax A, in spite of a nearly uniform distribution of electrons. The same tendency was found in several lobes of radio galaxies (Tashiro et al., 1998; Isobe et al., 2002; Comastri et al., 2003). Figure 2 apparently shows the relatively uniform brightness of the IC X-rays with a slight brightening toward the host galaxy in the east lobe of Fornax A, in contrast to the radio distribution. The X-ray and radio distribution imply a slight discrepancy between the spatial structures of the energy densities of electrons and magnetic field in the lobe. However the limited statistics of our *XMM-Newton* data prevent us from investigating in detail.

Table 2. Physical quantities in the lobes of Fornax A.

Parameters	East lobe	West lobe[a]
Radius(arcmin)	10	11
$S_{\rm R}$(Jy)[b]	44	50
$\Gamma_{\rm R}$[c]	1.68 ± 0.05	
$S_{\rm 1keV}$(nJy)	$90\ ^{+8}_{-9}$	100 ± 10
$B_{\rm me}(\mu{\rm G})$[d]	1.55	1.59
$B(\mu{\rm G})$	$1.23\ ^{+0.08}_{-0.06}$	1.22 ± 0.07
$u_{\rm m}(10^{-13}$ erg cm$^{-3})$	$0.60\ ^{+0.08}_{-0.06}$	$0.59^{-0.08}_{-0.06}$
$u_{\rm e}(10^{-13}$ erg cm$^{-3})$[e]	3.0 ± 0.3	$2.6^{+0.3}_{-0.2}$
$u_{\rm e}/u_{\rm m}$	$5.0\ ^{+1.1}_{-1.0}$	$4.4^{+1.1}_{-0.9}$

[a]The parameters re-evaluated after TEA01. [b]Flux density at 1.4 GHz. [c]Energy index of synchrotron radio emission. [d]Magnetic field calculated under the minimum energy condition, excluding proton contribution (Miley, 1980). [e]calculated for electrons with a Lorentz factor of $\gamma_{\rm e} = 10^3$ to 10^5.

ACKNOWLEDGMENTS

We thank Dr. I. Takahashi for his guidance of the *XMM-Newton* data analysis, especially the background estimation. This result is based on the observation obtained with *XMM-Newton*, an ESA science mission with instruments and contributions directly funded by ESA Member States and NASA.

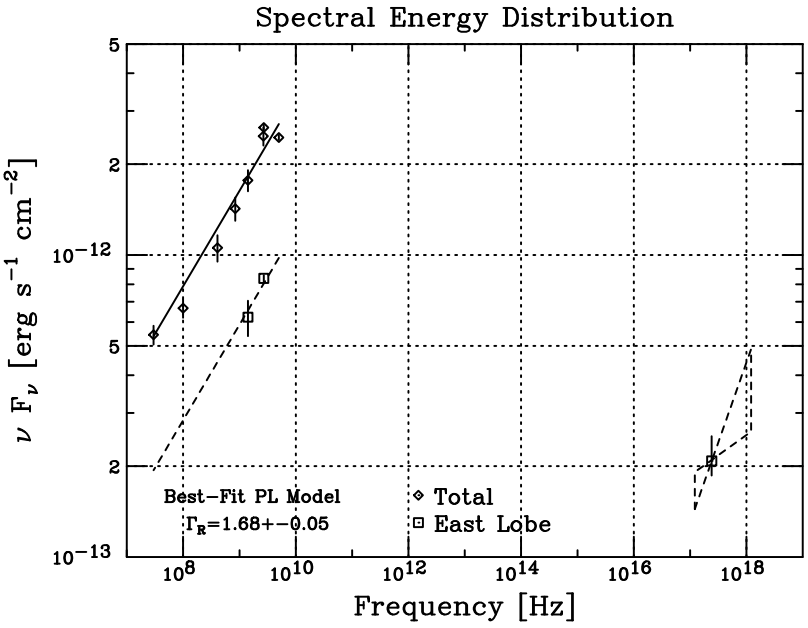

Figure 4. The spectral energy distribution of Fornax A. The diamonds and boxes refer to the data for the whole radio structure and those for the east lobe, respectively. The dashed tie represents the best-fit X-ray PL model of the east lobe. The solid line shows the best-fit PL model of $\Gamma = 1.68$ *to the radio spectrum of the whole structure, and the dashed one also shows the similar PL model, with the flux normalized by 0.36 to fit the east lobe spectrum. The radio data are taken from Ekers (1969), Ekers et al. (1983), Finlay & Jones (1973), Jones & McAdam (1992), Kühr et al. (1981), Robertson (1973), and Shimmins (1971)*

REFERENCES

Brunetti, G., Setti, G., & Comastri, A., 1997, A&A, 325, 898

Comastri, A., Brunetti, G., Dallacasa, D., Bondi, M., Pedani, M., Setti, G., 2003, MNRAS, 304, L52

Croston, J.H., Hardcastle, M.J., Harris D.E., Belsole, E., Birkinshaw, M., & Worrall, D. M., 2005, ApJ, 626, 733

Ekers, J.A., 1969, Australian J. Phys. Suppl., 7, 3

Ekers, R.D., Goss, W.M., Wellington, K.J., Bosma, A., Smith, R.M., & Schweizer, F., 1983, A&A, 127, 362

Feigelson, E.D., Laurent-Muehleisen, S.A., Kollgaard, R.I., & Fomalont, E.B., 1995, ApJ, 449, L149

Finlay E.A., & Jones B.B., 1973, Australian J. Phys., 26, 389

Fomalont, E.B., Ebneter, K.A., van Breugel, W.J.M. & Ekers, R.D., 1989, ApJ, 346, L17

Harris, D.E., and Grindlay, J.E., 1979, MNRAS, 188, 25

Isobe, N, Makishima, K., M., Tashiro, & S. Hong 2005, ApJ, 632, 781

Isobe, N., et al., 2002, ApJ, 581, L111

Isobe, N., Makishima, K., Tashiro, M., Itoh, K., Iyomoto, N., Takahashi, I., & Kaneda, H., submitted to ApJ.

Iyomoto, N. Makishima, K., Tashiro, M., Inoue, S., Kaneda, H., Matsumoto, Y., & Mizuno, T., 1998, ApJ, 503, 31

Jones, P.A., McAdam, W.B., 1992, ApJS, 80, 137

Kaneda, H., Tashiro, M., Ikebe, Y., Ishisaki, Y., Kubo, H., Makshima, K., Ohashi, T., Saito, Y., et al. 1995, ApJ, 453, L13

Kim, D-W, & Fabbiano, G., 2003, ApJ, 586, 826

Kühr, H., Witzel, A., Pauliny-Toth, I.I.K., & Nauber, U., 1981, A&AS, 45, 367

Madore, B.F., et al., 1999, ApJ, 515, 29

Miley, G., 1980, ARA&A, 18, 165

Robertson, J.G., 1973, Australian J. Phys., 26, 403

Shimmins, A.J., 1971, Australian J. Phys. Astrophys. Suppl., 21, 1

Stark, A.A., Gammie, C.F., Wilson, R.W., Bally, J., Linke, R.A., Heiles, C. & Hurwitz, M., 1992, ApJS, 79, 77

Tashiro, M., et al., 1998, ApJ, 499, 713

Tashiro, M., Makishima, K., Iyomoto, N. Isobe, N., & Kaneda, H. 2001, ApJ, 546, L19